Future increases in Amazonia water stress from CO_2 physiology and deforestation

Yue Li[1,*], Jessica C.A. Baker[2], Paulo M. Brando[3,4], Forrest M. Hoffman[5], David M. Lawrence[6], Douglas C. Morton[7], Abigail L.S. Swann[8,9], Maria R. Uribe[3], James T. Randerson[1]

[1]Department of Earth System Science, University of California, Irvine, CA, USA

[2]School of Earth and Environment, Leeds University, Leeds, UK

[3]Yale School of the Environment, Yale University, New Haven, CT, USA

[4]Instituto de Pesquisa Ambiental da Amazônia (IPAM), Brasília-DF, Brazil

[5]Climate Change Institute, Oak Ridge National Laboratory, Oak Ridge, TN, USA

[6]National Center for Atmospheric Research, Boulder, CO, USA

[7]NASA Goddard Space Flight Center, Greenbelt, MD, USA

[8]Department of Atmospheric Sciences, University of Washington, Seattle, WA, USA

[9]Department of Biology, University of Washington, Seattle, WA, USA

[*]Corresponding author: yue.li@uci.edu

Several different drivers are contributing to climate change within the Amazon basin, including forcing from greenhouse gases and aerosols, plant physiology responses to rising CO_2, and deforestation. Attribution among these drivers has not been quantified for shared socioeconomic pathway (SSP) climate simulations. Here, we identify the contribution of CO_2 physiology and deforestation to future hydroclimate change in the Amazon basin by combining information from three experiments and eight different Earth system models in CMIP6. Together, forcing from CO_2 physiology and deforestation account for about 44% of the projected annual precipitation decline, 48% of surface relative humidity decline, and 11% of warming over the Amazon basin by 2100 for SSP3-7.0. Other CMIP6 SSP simulations have similar contributions from the two drivers. Insight from our attribution analysis can aid in identifying research priorities aimed at reducing uncertainty in future projections of water availability, carbon dynamics, and wildfire risk.

Climate change is a major threat to Amazon rainforests as warming and drying contribute to higher levels of tree mortality in intact forests[1,2] and to more destructive fires that escape human control[3,4]. To explore both future climate change and its impacts within the Amazon basin, Earth system model (ESM) simulations from the 5th and the 6th Phases of the Coupled Model Intercomparison Project (CMIP)[5-12] are widely used. Specifically, simulations from ScenarioMIP[13] for different future shared socioeconomic pathway (SSP)[14] scenarios have been analyzed extensively to assess climate change impacts on ecosystem composition[15], carbon storage[16], the hydrological cycle[17], fire risk[18], and socio-economic systems[19], often with the

CMIP simulations serving as external forcing for a set of downstream models that resolve the basin with a higher spatial resolution or greater process representation (for example, Koch & Kaplan[16]). Another important application of the CMIP simulations is their use in the development of emergent constraints[20], which allow for a better understanding of the individual models from the broader ensemble that are more likely to accurately predict the sign and magnitude of future change[21-23]. Despite the extensive use of SSP simulations for these purposes, we do not clearly understand how different forcing agents within the simulations contribute to projected future changes in climate and the hydrological cycle in the Amazon basin.

Identifying the forcing agents responsible for projected future changes in climate is important for identifying research priorities to reduce uncertainties in key model components. In CMIP6 SSP simulations, critical forcing agents include well mixed greenhouse gases, aerosols, and land use change. Particularly for the Amazon basin, it is well established that the surface evapotranspiration changes from plant stomatal responses to rising atmospheric CO_2 and deforestation are important drivers of the precipitation response[24-29], yet studies analyzing SSP simulations may include an implicit assumption that most of the projected change in the basin is associated with the climate system response to radiative forcing from greenhouse gases and aerosols, since these are the main forcing agents at a global scale (for example, Zhao & Dai[12]). To ensure a successful and informative assessment for policy- and decision-makers, it is essential to provide comprehensive reports on both the magnitude of climate change and its consequences. Additionally, it is crucial to clearly quantify the factors that contribute to future regional change. Failing to fully understand these key drivers hinders progress in reducing uncertainties within climate models[30].

Future precipitation changes in Amazonia will likely be influenced by increased atmospheric CO_2 and deforestation[31,32]. The CO_2 impacts on Amazonian precipitation can be separated into radiative and plant physiological effects. The CO_2 radiative effect alters physical and dynamical processes, with regional Amazonian precipitation responding to large-scale thermodynamical adjustments of the ocean-atmosphere system, including the “wet regions getting wetter” mechanism identified in past work[33,34]. By contrast, the plant physiological effect in response to rising CO_2 is associated with a reduction in plant stomatal conductance and land surface evapotranspiration, that in turn, influence boundary layer processes, the frequency of deep convection, and interactions with the tropical jet[35]. Though sharing similar mechanisms of reducing surface evapotranspiration and boundary layer humidity, deforestation additionally increases surface albedo and reduces surface roughness, two processes that play major roles in altering precipitation patterns in various parts of the Amazon basin[36-38]. Across the basin as a whole, it has been suggested that increasing the deforestation fraction may cause a linear decline in regional average precipitation[39], and that for some scenarios of future change, this decline in precipitation may be similar in magnitude to that caused by forcing from CO_2 physiology[40].

Despite the well-understood mechanisms of the rainfall reductions due to CO_2 physiology[25,35,40] and deforestation[41], there remains a lack of comprehensive and quantitative understanding of their contributions to future rainfall and other climate variable changes in future (21st century) simulations conducted as a part of ScenarioMIP for different SSPs. This attribution is challenging, in part, because each SSP has a different level of atmospheric CO_2 and prescribed forest cover change. In this study, we attribute changes in Amazonian precipitation, surface relative humidity, and climate warming in the SSP simulations to forcings from CO_2 physiology and deforestation. For this purpose, we analyzed idealized model simulations from two model comparison projects (MIPs) that were undertaken as a part of CMIP6 (see Methods), namely, the Coupled Climate–Carbon Cycle Model Intercomparison Project (C4MIP[42]) and the Land-Use Model Intercomparison Project (LUMIP[43]). Idealized experiments of the land surface response to rising CO_2 in C4MIP (known as the biogeochemically coupled or BGC simulations) and to deforestation in LUMIP enabled us to first quantify the climate response of Amazon rainforest to these two mechanisms under uniform simulation protocols. We specifically analyzed transient simulations from eight models participating in C4MIP and six models participating in LUMIP (Supplementary Tables 1 and 2). This analysis revealed that regional annual mean precipitation, surface relative humidity, and air temperature respond linearly to atmospheric CO_2 concentration and forest cover fraction in the Amazon basin. In a second step, we applied linear models of the climate response to the absolute change in CO_2 concentration or forest cover fraction to quantify the contribution of these mechanisms to climate change in the Amazon basin for different CMIP6 SSP simulations.

Isolating climate response to rising CO_2 or deforestation

We find that for the influence of rising CO_2 on plant physiology, the models show a significant (and mostly linear) decline in mean annual precipitation of -0.91 ± 0.07% ($P < 0.001$, t-test) for a CO_2 increase of 100 ppm (Fig. 1a). Multiplied by the quadrupling increase in CO_2 (that is, from 285 ppm to 1140 ppm between last and first 20 years of the C4MIP BGC simulations) and a basin-wide mean annual precipitation climatology of 6.1 mm d^{-1}, this precipitation response to the CO_2 physiological forcing is equivalent to -0.47 mm d^{-1}, which is broadly consistent with estimates for this response from the mean of previous CMIP5 models (for example, -0.48 mm d^{-1} in Kooperman et al. [25]). We also find all the individual CMIP6 models used in this study show a significant negative precipitation response to CO_2 physiological forcing (ranging from -0.5% to -1.6% per 100 ppm CO_2 increase), highlighting a reasonably coherent response of Amazonian precipitation to CO_2 physiological forcing within CMIP6 (Supplementary Table 2).

Deforestation also significantly decreases mean annual precipitation in the Amazon basin (Fig. 1b). The multi-model average response is -1.0 ± 0.3% per 10% deforestation ($P < 0.001$), relatively linear, and equivalent to about 10% or -0.61 ± 0.18 mm d^{-1} for 100% (complete) deforestation of the whole basin. The sign and magnitude of the multi-model average precipitation response from the fully coupled LUMIP simulations for complete deforestation is nearly identical and with a lower uncertainty compared to the mean estimate of -12 ± 11% (per 100% deforestation) from a recent meta-analysis synthesizing information from climate models with various degrees of ocean, ice, and atmospheric coupling[39]. Moreover, we find all models agree on the sign of the response with their magnitude ranging from -0.15% to -2.3% in response to a 10% loss of forest cover, despite important structural differences in the CMIP6 models with respect to the representation of vegetation-hydrology coupling and biophysical responses to land use change[28,29].

Spatially, the precipitation response to forcing from a 100 ppm CO_2 increment is strongest in the northeastern part of the basin (Fig. 2a), with a pattern consistent with previous reports[34]. Whereas the climate response to the basin-wide 10% deforestation is strongest in central and western Amazonia, adjacent to the Andes Mountain range (Fig. 2b). Further, the CO_2 physiological forcing and deforestation also influence seasonality of the precipitation response. Across the annual cycle, the CO_2 physiology impacts on precipitation are somewhat uniform, when expressed as a percent change. However, the precipitation response in the southeastern part of the basin is stronger toward the end of the dry season (August and September) than at the beginning of the dry season (June and July) (Supplementary Fig. 1). The negative precipitation response to deforestation appears to be most robust across the models during the wet season (December to May), although there is also a strong response and high level of agreement across models in the northern and eastern part of the basin during August, September, and October (Supplementary Fig. 2).

The negative precipitation response to forcing from CO_2 physiology and deforestation implies greater future risks for meteorological drought and fire. To provide more insight into potential changes in these risks caused by CO_2 physiology and deforestation forcing, we performed a similar regression analysis (see Methods) for surface relative humidity (RH) from the five models with available output from C4MIP and the four models with available output from LUMIP. Basin-wide RH decreases at a rate of -0.91 ± 0.02% ($P < 0.001$) in response to a 100 ppm CO_2 increase and by -0.5 ± 0.1% ($P < 0.001$) in response to a 10% loss of tree cover in the Amazon basin (Fig. 1c, d). Regressions for each available model also confirm that the RH response is consistently negative in response to these drivers, although not every model exhibits a statistically significant trend (Supplementary Table 2). The spatial pattern of RH response to CO_2 physiology and deforestation is more homogeneous than for precipitation, with the largest signal occurring in the central Amazon basin (Supplementary Fig. 3a, b).

Similar to precipitation and RH, the surface air temperature response in the Amazon basin to forcing from CO_2 physiology is mostly linear (Fig. 1e), with a regional average warming rate of 0.13 ± 0.01 °C per 100 ppm increase in CO_2 ($P < 0.001$). All models agree on a significantly positive surface air temperature response to rising CO_2 (Supplementary Table 2). This warming signal is likely to increase the saturation vapor pressure, which, combined with the declined surface moisture availability due to declined stomatal conductance, contributes to the RH declines for CO_2 physiology.

The surface air temperature response to deforestation is considerably noisier than for the other climate variables shown in Figure 1f, with a 10% loss in forest fraction contributing to a basin-scale warming of 0.03 ± 0.02 °C ($P = 0.058$). Further regression analysis was performed for each model, revealing that the sign and magnitude of deforestation impacts on surface air temperature diverge considerably from model to model (-0.19 °C to 0.15 °C in response to 10% deforestation, Supplementary Table 2). Specifically, the CanESM2 and UKESM1 show decreases in surface air temperature from deforestation in contrast to the other models that show a warming trend (Supplementary Table 2). Some of this variation may be linked to cooling from deforestation in the extratropics in the LUMIP simulations (ref. [28]). As a result, the mean estimate of climate warming from deforestation reported here is likely a lower bound (that is, CanESM2 and UKESM1 contribute negatively to the ensemble mean warming, Supplementary Table 2) and has a high level of uncertainty associated with model-to-model variability (see Discussion for further information). Compared to the spatial pattern of the precipitation response, the spatial patterns for the warming response to CO_2 physiology and deforestation are diffuse and broadly similar, with the strongest response in the central part of the basin (Supplementary Fig. 3c, d).

The climate responses to CO_2 physiology and deforestation are not directly comparable in Figs. 1 and 2, with the slopes having different units. However, we can compare relative impacts of the two drivers by specifying a fixed increment of atmospheric CO_2 and then identifying the equivalent level of deforestation necessary to generate the same magnitude of climate change. For precipitation, a 100 ppm CO_2 increase is equivalent to a 9% increase in deforestation in terms of generating an equivalent amount of climate change for the set of CMIP6 models analyzed here. Similarly, for relative humidity a 100 ppm CO_2 increase is equivalent to an 18% increase in deforestation, and for temperature, a 100 ppm CO_2 increase is equivalent to a 43% increase in deforestation.

Contributions of CO_2 physiology and deforestation in SSPs

The analysis shown in Figure 1 provides evidence that the climate response to atmospheric CO_2 concentration or deforestation is mostly linear in CMIP6 models for the domain of the Amazon basin. As a next step, we used these linear relationships to separately isolate climate change arising from these two drivers in widely used SSP scenarios[13] by the end of the 21st century. We estimated their contributions as the product of the multi-model average climate response from Fig. 1 and the changes in future atmospheric CO_2 concentration or deforestation fraction from each SSP simulation (Fig. 3, Methods). Contributions from the CO_2 physiology and deforestation have not been systematically identified for ScenarioMIP SSP simulations that integrate the forcing from many different climate change drivers.

SSP scenarios have different pathways of future atmospheric CO_2 concentration and land use, depending on different assumptions about the strength of international cooperation, technology, and economic development[14]. SSP1-2.6 has been described as the most sustainable future with global temperature stabilizing below 2°C of warming by 2081-2100 (ref. [44]). In this scenario, atmospheric CO_2 increases slowly, reaching a maximum of 474 ppm in 2063, and then declining to a mean level of 456 ppm by 2081-2100. By contrast, atmospheric CO_2 concentrations under the other three scenarios keep rising throughout the 21st century, reaching 597 ppm for SSP2-4.5, 792 ppm for SSP 3-7.0, and 1005 ppm for SSP5-8.5. The CO_2 increments for these SSPs, relative to the background level in 1850 for the pre-industrial control, are summarized in Fig. 3.

Although SSP5-8.5 has the highest atmospheric CO_2 increase, its assumptions regarding global energy development are not closely coupled to land use change, and therefore the deforestation fraction in the Amazon basin remains nearly constant at 6.4% from 2021-2040 through 2081-2100. This projection is similar to the 6.1% deforestation fraction for SSP1-2.6. For SSP2-4.5, Amazonian deforestation first increases to 8.3% during 2041-2060 and then decreases to 5.2% during 2081-2100 as a consequence of forest recovery (Fig. 3b). The greatest Amazonian forest cover loss occurs under SSP3-7.0 where deforestation increases to 12.4% by 2081-2100 (Fig. 3c).

Precipitation decreases by 4.8% (-0.26 mm d^{-1}) for SSP1-2.6 by 2081-2020 relative to the pre-industrial mean level in 1850 (5.5 mm d^{-1}). For this scenario, we find that the sum of contributions from CO_2 physiology and deforestation account for 46% (-0.12 mm d^{-1}) of future precipitation decline over the Amazon basin (Fig. 4a). Similarly, of the 13.2% decline (-0.72

mm d^{-1}) in Amazonia precipitation occurring by 2100 for SSP3-7.0, 44% of this decrease (-0.32 mm d^{-1}) can be attributed to the combined effect of CO_2 physiology and deforestation. Across all the different future scenarios and time intervals shown in Fig. 4, the combined contributions of CO_2 physiology and deforestation to Amazonian precipitation change vary between 34% and 56% (Fig. 4). For surface RH, a key driver of fire risk[45,46], the impact of CO_2 physiology and deforestation is even greater in magnitude, accounting for 48% of the RH decline for SSP3-7.0 and 52% for SSP5-8.5 (Supplementary Fig. 4). These findings highlight the importance of decreases in surface evapotranspiration due to both CO_2 physiology and deforestation (Supplementary Fig. 5a, b) as key model drivers influencing the future hydroclimate of the Amazon basin (Fig. 5).

In contrast, for surface air temperature, the contribution from the two drivers to warming is relatively small, primarily because of the stronger regional and global temperature response to radiative forcing from greenhouse gases. For example, for SSP3-7.0 about 11% of future Amazonian warming can be attributed to forcing from CO_2 physiology and deforestation by the end of the century (Fig. 5, Supplementary Fig. 6).

Solely considering contributions from the response of physiology to rising CO_2, precipitation declines ranged between 33% for SSP1-2.6 to 46% for SSP5-8.5 (Fig. 4a, d). Deforestation contributions to precipitation declines varied between 4% for SSP5-8.5 to 13% for SSP1-2.6. CO_2 physiology also had a much larger impact than deforestation for relative humidity and temperature changes within the different SSP simulations.

Discussion

CO_2 physiology and deforestation are found to account for over 40% of the declines in both precipitation and surface relative humidity in the Amazon basin by the end of the 21st century (Fig. 4, Supplementary Fig. 4). These results indicate that a considerable amount of future Amazonian precipitation and meteorological drought[7-12] can be attributed to drivers other than the radiative effects of greenhouse gases and aerosols. The important role of climate forcing from the land surface could enable a relatively fast (and positive) hydroclimate response in the Amazon basin if climate policies are enacted that allow for reforestation or a decline in atmospheric CO_2 levels. This contrasts with the considerably slower (multi-decadal) response time of climate to radiative forcing from greenhouse gases as a consequence of long-term adjustments in ocean heating[47]. The estimated contributions of deforestation to future precipitation at the basin scale vary between 4% and 13% across the different SSPs. These estimates also serve as a range for the potential co-benefits in hydroclimate that could be achieved by preventing further deforestation, complementing carbon and ecological co-benefits reported in previous work[48].

As a consequence of land-atmosphere interactions, past work has identified a loss of 40% of forest within the Amazon basin as a “tipping point”, beyond which hydroclimate changes would threaten the viability of remaining forests[31]. Our analysis also points to the negative consequences of deforestation for precipitation, but additionally suggests that at least for widely analyzed SSPs, threats to the future hydroclimate of the Amazon basin are even larger from the radiative effects of greenhouse gases and aerosols and from direct ecosystem responses to rising levels of atmospheric CO_2.

The significant contributions of CO_2 physiology to future Amazonian precipitation change in CMIP6 SSP simulations highlight the importance of improving our knowledge on key processes of vegetation effects on precipitation and meteorological drought within the Amazon basin[49]. We have shown in this study the model evidence of rising CO_2 impacts on evapotranspiration, albedo, and leaf area index (Supplementary Fig. 5a, c, e). More observational and model explorations are needed to understand the resulting changes in boundary layer, deep convection, and regional circulation in order to reduce model uncertainties. While CMIP models provided a coherent and robust response to CO_2 forcing associated with plant physiology, the magnitude of this response remains highly uncertain mainly because there are relatively few ecosystem-level observations from tropical forests available for model testing. This highlights the importance of new, sustained stomatal conductance and evapotranspiration measurements at different CO_2 levels, such as those planned as a part of the Amazon FACE experiment[50]. Additionally, acclimation of stomatal conductance responses to long-term increasing levels of atmospheric CO_2 remains a key unresolved issue in this respect[51].

Other key process-based uncertainties include the representation of land-atmosphere coupling and atmospheric convection that influence the precipitation recycling ratio in the Amazon basin[52], and the ability of the models to capture the influence of changing ocean dynamics on future atmospheric circulation (and precipitation). For example, a recent study reported there is a systematic bias in CMIP6 models in capturing the cooling signal over the eastern equatorial Pacific in the past four decades[53]. Such a cooling pattern resembles a La-Niña-like condition that could increase the precipitation in the Amazon basin through changes in local Walker circulation[54]. Some of the model-to-model differences in the magnitude of the

SSP precipitation response (shown with the error bars in Fig. 4, Supplementary Table 3) can likely be traced back to the ocean response to radiative forcing from greenhouse gases and aerosols[55,56], which also needs further exploration in future work.

For deforestation, paths for reducing uncertainty in coupled model estimates of the Amazonian climate response include more extensive comparison of models with observations and refinement of the LUMIP protocol for CMIP7. In this study, we report that the local biophysical temperature effects range from -0.19 °C to 0.15°C in response to 10% deforestation in the Amazon basin (Supplementary Table 2). Although the multi-model mean warming response is consistent with past work[41], variability in the magnitude of the response across the different CMIP models is large and stems from at least three possible sources. First, there is a difference in the level of calibration and validation efforts from each modelling group to improve the biophysical temperature effects of deforestation. For example, land component of CESM2, the Community Land Model (CLM), has been improved through parameter optimization[57] and benchmarking with satellite observations[58]. Second, there are still a limited number of observations in the Amazon basin to help with the model calibration. For instance, a recent comparison of biogeochemical and biophysical climate effects of deforestation[59] includes observational datasets from Bright et al. [60] and Duveiller et al. [61], which are still limited to a paucity of paired forested and non-forested eddy-covariance sites and relatively sparse satellite data coverage due to frequently cloudy conditions. Third, the CMIP6 LUMIP deforestation protocol is global in scope[28]. In designing the future LUMIP protocol for CMIP7, consideration of a tropical-only experiment with an increased number of ensemble members may provide a stronger basis for robustly characterizing regional climate responses. Further analysis of drought and fire metrics in LUMIP simulations, including soil moisture and burned area, is also needed to understand better the processes of regional-scale dynamic vegetation feedbacks to Amazonian hydroclimate from changes in forest cover.

By recognizing the relatively fast adjustment time and linear relationship between land surface forcing and Amazonian climate response, we developed a first attempt to separate CO_2 physiology and deforestation contributions to climate change in CMIP6 SSP simulations. While the assumption of linearity and independence of the two forcing agents simplified our analysis, it is important to recognize potential interactions and feedback between these two drivers and target these interactions in future work. Further deforestation, for example, may weaken the regional climate response to rising CO_2 as forests are replaced with pastures and grasslands that have a smaller roughness and canopy fraction for transpiration. Across the SSPs, the deforestation fraction is generally small, as predicted in the SSPs by the end of the 21st century and ranges from 5.2% in SSP-2-4.5 to 12.4% in SSP3-7.0. To estimate the potential magnitude of some of these interactions, we performed a back-of-the-envelope calculation. Specifically, for the SSP3-7.0 scenario, we reduced the CO_2 physiological contribution by 12% to reflect the concurrent loss of total forest cover. With this simple assumption, which is likely an upper bound due to the largest deforestation fraction of 12%, the precipitation decline attributed to CO_2 physiology decreases from 35% to 31%. Some additional non-linearities are likely to be introduced from interactions between the radiative effects of greenhouse gases and the land surface forcing mechanisms explored here. Supplementary Fig. 7, for example, shows that CO_2 physiology effect on precipitation is largely independent of the deforestation effect but has a weak relationship with precipitation response to CO_2 radiative effect. These illustrative calculations and analysis suggest that interactions may slightly reduce our estimated magnitude of precipitation effects but are unlikely to change our study's main findings qualitatively. This also highlights the need to explore feedback between forcing agents in future work. One effective way to accomplish this in CMIP7 would be to add a CO_2 physiology simulation (for example, a BGC simulation) and a land use simulation to the DAMIP[62] for historical and 1-2 SSPs to 2100.

In this study we provide an attribution analysis of Amazonian climate change in widely used SSP simulations by isolating contributions from the plant physiological response to rising CO_2 and deforestation. We accomplish this by combining information from two different idealized experiments from CMIP6. From the idealized (biogeochemically-coupled) CO_2 experiment from C4MIP and the idealized deforestation experiment from LUMIP, we identify that the climate change response to feedbacks from changes in the land surface are rapid and mostly linear across the basin and across the dynamic range of CO_2 concentration and land cover change captured by the SSPs. The combined effects from the two drivers account for more than 40% of future basin-wide precipitation and surface relative humidity declines, but less than 11% of warming over the Amazon basin by the end of the 21st century. This implies a substantial contribution from CO_2 physiology and deforestation to increasing risk of future meteorological drought and wildfire. Our findings provide insight about the sources of uncertainty of climate model projections and may help with identifying the full scope of climate benefits associated with forest conservation policies in the Amazon basin.

Methods

We isolated the climate change response in the Amazon basin to CO_2 physiology and deforestation using output from two idealized CMIP6 experiments. From C4MIP[42] we analyzed the idealized 140-year simulations (1pctCO2-bgc) in which CO_2 concentrations increase by 1% per year, but the CO_2 increases are not radiatively active (that is, all models' radiation code uses a constant atmospheric CO_2 concentration that was held constant at the pre-industrial level). The 1pctCO2-bgc experiment from C4MIP allows for the isolation of the climate response resulting from plant physiological responses to rising CO_2. From LUMIP[43] we analyzed a global idealized deforestation experiment (deforest-glob). The LUMIP deforest-glob simulation has an 80-year duration with a total forest area of 20 million km^2 linearly removed from each model's top 30% of forest grid cell across the globe during the first 50 years. This results in about a 0.9% per year decline in tree cover fraction across the Amazon basin as a whole (that is, the deforestation was mostly spatially homogeneous in the simulations). Since there are only deforestation effects in this experiment, changes in Amazonian climate can be attributed solely to this driver.

In a second step, we identified the contribution of plant physiology responses to rising CO_2 and deforestation to Amazonian climate change within CMIP6 future scenario experiments (ScenarioMIP)[13]. We focused on CMIP6 simulations for 4 widely used shared socioeconomic pathways (SSPs)[14]. These SSP simulations have different radiative forcing levels by 2100. They are: SSP1-2.6, SSP2-4.5, SSP3-7.0, and SSP5-8.5. The number behind each future scenario (for example, 8.5 for SSP5-8.5) indicates the radiative forcing level (unit: W/m^2) that occurs in the scenario by 2100. To quantify the relative change in Amazonian climate in the future, we also include the pre-industrial control (piControl) experiment of CMIP6 that uses fixed radiative forcing identical to the level during the year of 1850. The year of 1850 is also the reference year in our study.

Monthly air temperature (tas), precipitation (pr), surface relative humidity (hurs), and tree cover (treeFrac) during the historical and future periods from the above CMIP6 experiments were downloaded from the archive of Earth System Grid Federation (ESGF). Before analysis, all variables were remapped to a 1-degree grid using the bilinear interpolation method from Climate Data Operator (CDO[63]). Because not all CMIP6 modeling centers participated in all four experiments as described above, we chose to use eight models that have the maximum availability of these variables (Supplementary Table 1). They include BCC-CSM2-MR (Wu et al. [64]), CanESM5 (Swart et al. [65]), CESM2 (Danabasoglu et al. [66]), CNRM-ESM2-1 (Seferian et al. [67]), IPSL-CM6A-LR (Boucher et al. [68]), GISS-E2-1-G (Kelley et al. [69]), UKESM1-0-LL (Sellar et al. [70]), and MPI-ESM1-2-LR (Mauritsen et al. [71]). To obtain the most robust climate response to CO_2 physiology and deforestation as possible, climate variables were averaged for each model across ensemble members based on their availability in both the C4MIP and LUMIP experiments (Supplementary Table 1). The ensemble mean approach helps improve the signal-to-noise ratio of the climate response either to CO_2 physiology or deforestation in the Amazon basin considering the different influences from interannual variability from each model. Yet, it also relies on the mechanism coherence and traceability across these models. For future SSP scenarios, atmospheric CO_2 concentrations during the 21st century were obtained from the input datasets for Model Intercomparison Projects (input4MIPS) and their land use including the fraction of forest in the Amazon basin was obtained from the Land Use Harmonization dataset version 2 (LUHv2f, ref. [72]).

To isolate the precipitation response to either plant physiological response to increasing CO_2 or deforestation within the eight CMIP6 models, the relative precipitation changes in percent were computed relative to the pre-industrial average for each model in each experiment before determining the average across models. We used simple linear regression equations to describe the response of precipitation, surface relative humidity, and surface air temperature to CO_2 concentration and forest cover percentage.

$$Y = \alpha + \beta \times x$$

where y indicates the climate variables such as precipitation, surface relative humidity, or surface air temperature, x indicates either CO_2 concentration change or deforestation fraction over the Amazon basin. Β and α are the slope and y-intercept as estimated from the above equation, respectively. As shown in Fig. 1, the estimated β at the basin scale was used as the climate sensitivity to either CO_2 concentrations in C4MIP 1pctCO2-bgc or deforestation fraction in LUMIP deforest-glob. The y-axis intercept value in Fig. 1 may not be identical to 100% for precipitation and to 0 for surface air temperature, probably from the influence of the internal variability. We chose not to force the regressions through a specified y-axis intercept to avoid overestimating contributions from CO_2 physiology and deforestation in our attribution analysis. To assess the spatial pattern of the Amazonian climate response, we also performed the linear regression analysis for each model pixel.

To estimate the contribution of plant physiological response to CO_2 to future climate change in the Amazon basin, we first computed the changes in the atmospheric CO_2

concentration from the pre-industrial era (that is, 1850) to different future periods (that is, 2021-2040, 2041-2060, 2061-2080, and 2081-2100). We then multiplied this CO_2 change with the slope derived from the linear regression describing the response of each climate variable to atmospheric CO_2 concentration from the C4MIP 1pctCO2-bgc simulations (left column in Fig. 1). In the 1pctCO2-bgc simulations, land cover was held constant throughout the simulations at 1850 levels. Similarly, the deforestation contributions were computed as the product of the basin-scale average deforestation fraction from each of the future SSPs scenarios relative to 1850 forest cover, and the slope derived from the linear regression describing the response of each climate variable to Amazonian deforestation fraction from the LUMIP deforest-glob simulations (right column in Fig. 1). In the LUMIP simulation atmospheric CO_2 concentration was held constant at 1850 levels[43]. The regression approach was applied for the purpose of deriving the sensitivity of the climate response to CO_2 concentration or deforestation fraction, respectively, using the different C4MIP and LUMIP simulations. The contribution by either CO_2 physiology or deforestation was estimated for the whole Amazon basin as shown in Fig. 4, Supplementary Figs. 4 and 6.

We assumed that the climate response to CO_2 physiological forcing and deforestation could be isolated from the CMIP6 simulations because climate responses to land surface forcing, including adjustments in boundary layer height and convection from changes in surface evapotranspiration, are known to be relatively fast, occurring over timescales of days to weeks[35].

Data availability

All CMIP6 simulations used in this study are publicly available at https://esgf-node.llnl.gov/projects/cmip6/. Atmospheric CO_2 concentrations for future SSP scenarios were downloaded from https://esgf-node.llnl.gov/projects/input4mips/. Future land use datasets LUHv2f were downloaded from https://luh.umd.edu/data.shtml.

Code availability

All computer codes used in this study are available via GitHub at https://github.com/YueLi92/Contributions_CO2Phys_Def_SSP.

Acknowledgement

Y.L. and J.T.R. acknowledge support from the U.S. Department of Energy (DOE) Office of Science, Biological and Environmental Research (BER), Earth and Environmental Systems Modeling program to study dust and fire (DE-SC0021302) and the RUBISCO Scientific Focus Area. J.T.R. and D.C.M. received funding support from NASA's SERVIR and MAP research programs. A.L.S.S. recognizes funding support from DOE BER Regional and Global Model Analysis program (DE-SC0021209). The funders had no role in study design, data collection and analysis, decision to publish or preparation of the manuscript.

Author Contributions Statement

Y.L. and J.T.R. designed the research; Y.L. performed data analysis and figure illustrations; Y.L. and J.T.R. drafted the manuscript, with discussions and contributions from J.C.A.B.,

P.M.B., F.M.H., D.M.L., D.C.M., A.L.S.S., M.R.U.; All authors reviewed and revised the manuscript.

Competing Interests Statement

The authors declare no competing interests.

Figure Captions

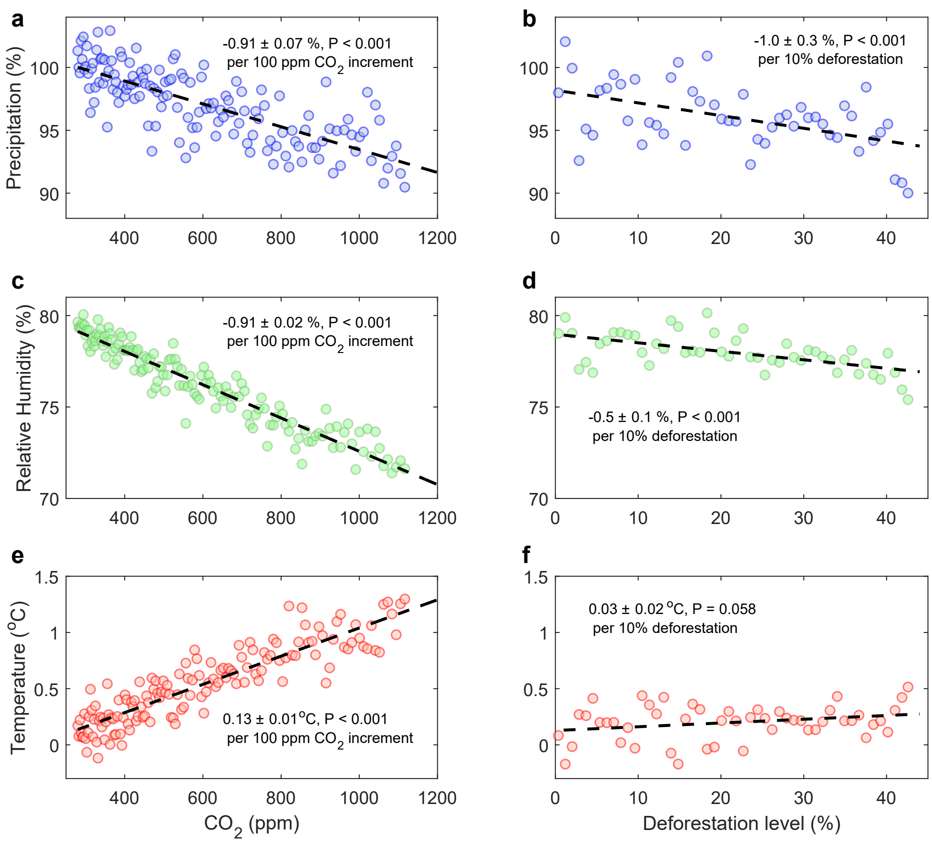

Figure 1. Transient response of annual mean precipitation, surface relative humidity, and air temperature to CO_2 physiology and deforestation in the Amazon basin. The precipitation changes were computed in percentage from each model, and then averaged across

eight CMIP6 models. Each data point represents the cross-model regional average that was computed for each year from their 140-year and 50-year simulations from the C4MIP and LUMIP experiments, respectively (see Methods). Climate changes are solely due to CO_2 physiology (no radiative effects) in the left column and deforestation in the right column. The exact *P* values for regression slope by t-test are 4.5×10^{-28} for (**a**), 2.1×10^{-4} for (**b**), 8.8×10^{-73} for (**c**), 6.0×10^{-6} for (**d**), 9.4×10^{-51} for (**e**), and 0.058 for (**f**).

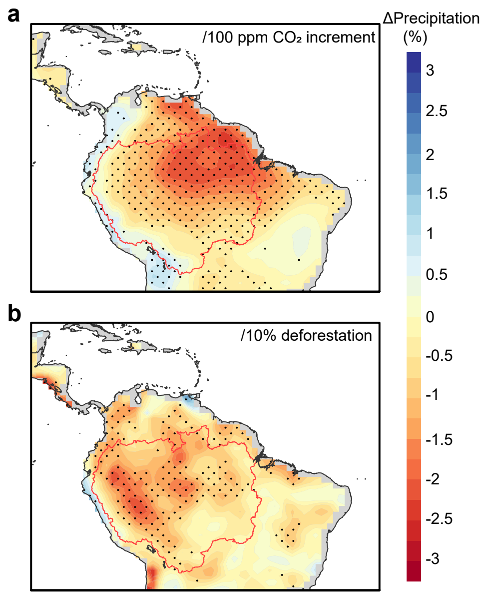

Figure 2. Spatial distribution of the mean annual precipitation response to forcing from CO_2 physiology and deforestation. Precipitation response to (**a**) 100 ppm CO_2 increase, (**b**) 10% loss in forest fraction. The precipitation changes were computed in percent from each model, and then averaged across CMIP6 models. Linear regressions were performed for the precipitation at each pixel against (**a**) atmospheric CO_2 concentrations and (**b**) basin-scale average in forest cover loss from their 140-year and 50-year simulations of the C4MIP and LUMIP experiments, respectively (see Methods). Dotted area indicates the model agreement,

with at least six out of eight models agreeing on the sign of the precipitation response.

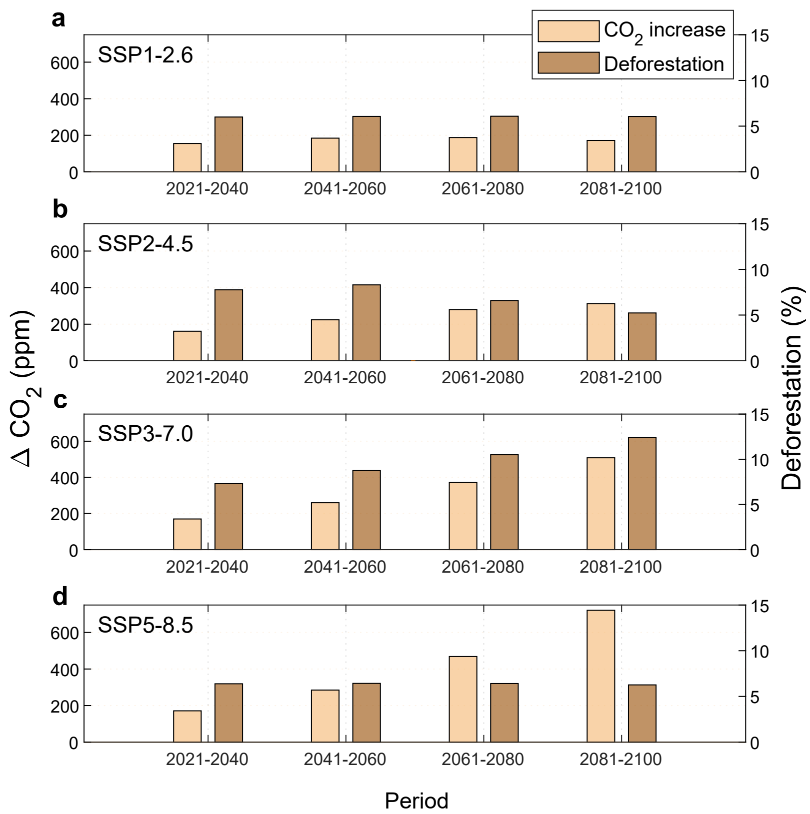

Figure 3. Changes in CO_2 concentrations and deforestation fraction of the Amazon basin in Shared Socioeconomic Pathways (SSPs). Both CO_2 increase (light brown) and loss in forest fraction of the Amazon basin (red brown) were computed as the difference between future projections and the preindustrial levels for (**a**) SSP1-2.6, (**b**) SSP2-4.5, (**c**) SSP3-7.0, and (**d**) SSP5-8.5. Future projections were derived from CMIP6 ScenarioMIP for different future shared socio-economic pathways (SSPs).

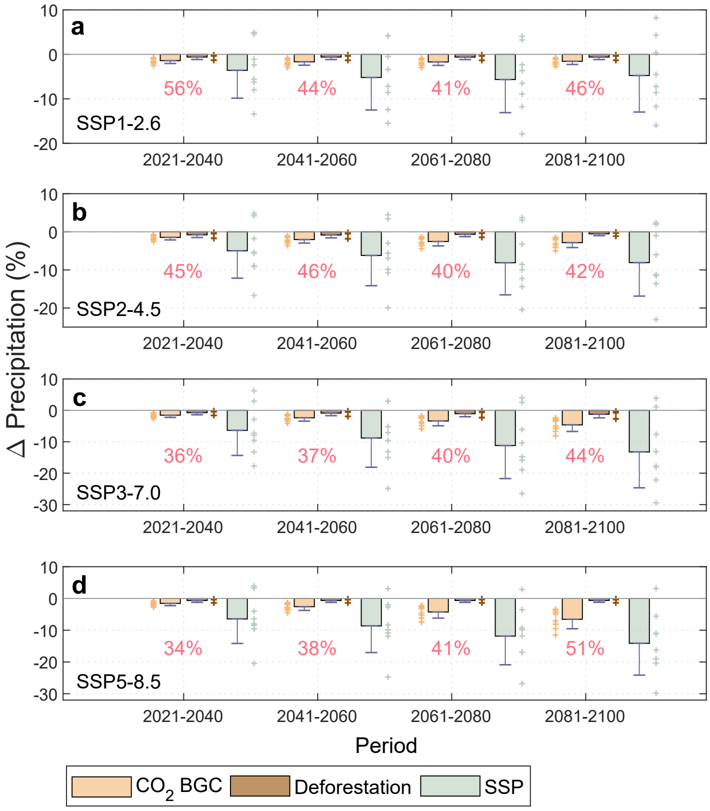

Figure. 4 Climate contributions of CO_2 physiology and deforestation to future changes in precipitation over the Amazon basin. Future changes in Amazonian precipitation (%) due to CO_2 physiological effects (light brown) and deforestation (red brown) were computed from the precipitation response from these two drivers (see Methods). Light grey indicates the future Amazonian precipitation changes under the four Shared Socioeconomic Pathways (SSPs) during different periods. They are: (**a**) SSP1-2.6, (**b**) SSP2-4.5, (**c**) SSP3-7.0, and (**d**) SSP5-8.5. Red numbers indicate the percentage of total precipitation changes for each time period and SSP attributed to CO_2 physiology and deforestation. Each error bar indicates 1 standard deviation (SD) being added to the mean values across the CMIP6 models with available output ($n = 8$ for CO_2 physiology and SSP simulation, $n = 6$ for deforestation). Data point for each model has been shown along with the bar as indicated by plus sign. Relative precipitation

changes in percent can be converted to absolute changes in mm d^{-1} by being multiplied by a multi-model mean annual precipitation of 5.5 mm d^{-1} for the pre-industrial period.

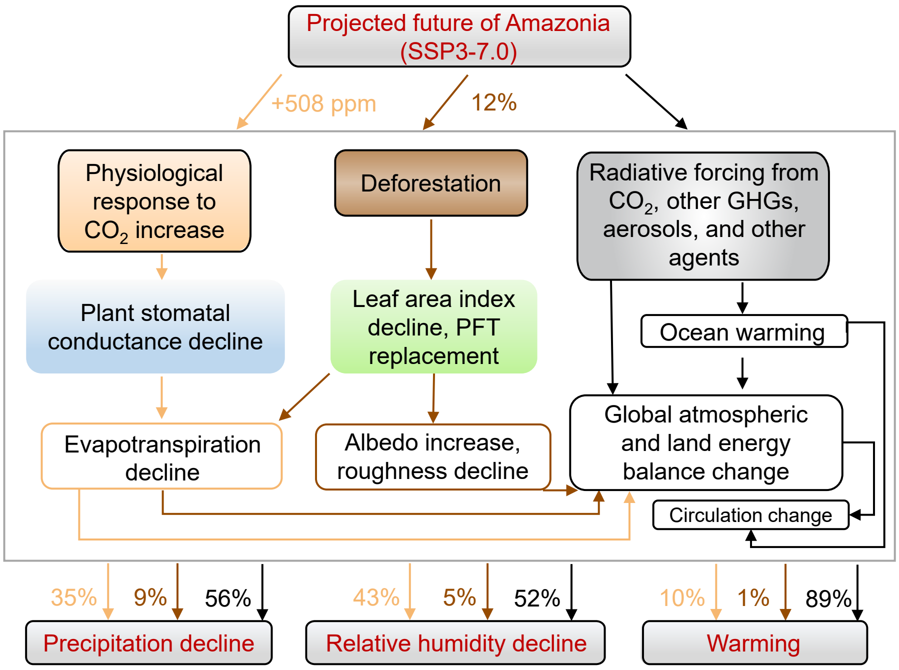

Figure 5. Schematic diagram of the mechanisms by which CO_2 physiology and deforestation influence climate change in the Amazon basin. Taking the SSP3-7.0 as an example, the contributions of CO_2 physiology and deforestation to Amazonian climate change by the end of the 21st century (2081-2100) were quantified using CMIP6 idealized experiments as described in the methods. More information about evapotranspiration, albedo, and leaf area index model responses, which play a key role in regulating the integrated climate response, can be found in Supplementary Fig. 5. Additional analysis of the underlying mechanisms can be found in previous work by Swann et al. [24], Zhou et al. [27], and Boysen et al. [28].

References

Cited in main text:

1. Malhi, Y. et al. Exploring the likelihood and mechanism of a climate-change-induced dieback of the Amazon rainforest. *Proc. Natl. Acad. Sci. U.S.A.* **106**, 20610-20615 (2009).
2. Phillips, O. L. et al. Drought sensitivity of the Amazon rainforest. *Science* **323**, 1344-1347 (2009).
3. Brando, P. M. et al. Abrupt increases in Amazonian tree mortality due to drought–fire interactions. *Proc. Natl. Acad. Sci. U.S.A.* **111**, 6347-6352 (2014).
4. Aragão, L. E. et al. 21st Century drought-related fires counteract the decline of Amazon deforestation carbon emissions. *Nat. Commun.* **9**, 1-12 (2018).
5. Orlowsky, B. & Seneviratne, S.I. Elusive drought: uncertainty in observed trends and short-and long-term CMIP5 projections. *Hydrol. Earth Syst. Sci.* **17**, 1765-1781 (2013).
6. Mankin, J.S., Seager, R., Smerdon, J.E., Cook, B.I. & Williams, A.P. Mid-latitude freshwater availability reduced by projected vegetation responses to climate change. *Nat. Geosci.* **12**, 983-988 (2019).
7. Cook, B.I., Mankin, J.S., Marvel, K., Williams, A.P., Smerdon, J.E. & Anchukaitis, K.J. Twenty-first century drought projections in the CMIP6 forcing scenarios. *Earth Future* **8**, e2019EF001461 (2020).
8. Parsons, L.A. Implications of CMIP6 projected drying trends for 21st century Amazonian drought risk. *Earth Future* **8**, e2020EF001608 (2020).

9. Ukkola, A.M., De Kauwe, M.G., Roderick, M.L., Abramowitz, G. & Pitman, A.J. Robust future changes in meteorological drought in CMIP6 projections despite uncertainty in precipitation. *Geophys. Res. Lett.* **47**, e2020GL087820 (2020).

10. Fan, X., Miao, C., Duan, Q., Shen, C. & Wu, Y. Future climate change hotspots under different 21^{st} century warming scenarios. *Earth Future* **9**, e2021EF002027 (2021).

11. Li, H. et al. Drylands face potential threat of robust drought in the CMIP6 SSPs scenarios. *Environ. Res. Lett.* **16**, 114004 (2021).

12. Zhao, T. & Dai, A. CMIP6 model-projected hydroclimatic and drought changes and their causes in the twenty-first century. *J. Clim.* **35**, 897-921 (2022).

13. O'Neill, B.C. et al. The scenario model intercomparison project (ScenarioMIP) for CMIP6. *Geosci. Model Dev.* **9**, 3461-3482 (2016).

14. Riahi, K. et al. The shared socioeconomic pathways and their energy, land use, and greenhouse gas emissions implications: an overview. *Glob. Environ. Change* **42**, 153-168 (2017).

15. Boit, A. et al. Large-scale impact of climate change vs. land-use change on future biome shifts in Latin America. *Glob. Chang. Biol.* **22**, 3689-3701 (2016).

16. Koch, A. & Kaplan, J.O. Tropical forest restoration under future climate change. *Nat. Clim. Chang.* **12**, 279-283 (2022).

17. Munia, H.A., Guillaume, J.H., Wada, Y., Veldkamp, T., Virkki, V. & Kummu, M. Future transboundary water stress and its drivers under climate change: a global study. *Earth Future* **8**, e2019EF001321 (2020).

18. Park, C.Y. et al. How Will Deforestation and Vegetation Degradation Affect Global Fire Activity?. *Earth Future* **9**, e2020EF001786 (2021).

19. Silva, M. V. M. D., Silveira, C. D. S., Cabral, S. L., Marcos Júnior, A. D., Silva, G. K. D., & Sousa, C. E. L. D. Naturalized streamflows and Affluent Natural Energy projections for the Brazilian hydropower sector for the SSP2-4.5 and SSP5-8.5 scenarios of the CMIP6. *J. Water Clim. Chang.* **13**, 315-336 (2021).

20. Hall, A. & Qu, X. Using the current seasonal cycle to constrain snow albedo feedback in future climate change. *Geophys. Res. Lett.* **33**, L03502 (2006).

21. Chen, Y., Langenbrunner, B. & Randerson, J.T. Future drying in Central America and northern South America linked with Atlantic meridional overturning circulation. *Geophys. Res. Lett.* **45**, 9226-9235 (2018).

22. Duffy, P.B., Brando, P., Asner, G.P. & Field, C.B. Projections of future meteorological drought and wet periods in the Amazon. *Proc. Natl. Acad. Sci. U.S.A.* **112**, 3172-13177 (2015).

23. Boisier, J.P., Ciais, P., Ducharne, A. & Guimberteau, M. Projected strengthening of Amazonian dry season by constrained climate model simulations. *Nat. Clim. Chang.* **5**, 656-660 (2015).

24. Swann, A.L., Hoffman, F.M., Koven, C.D. & Randerson, J.T. Plant responses to increasing CO_2 reduce estimates of climate impacts on drought severity. *Proc. Natl. Acad. Sci. U.S.A.* **113**, 10019-10024 (2016).

25. Kooperman, G.J. et al. Forest response to rising CO_2 drives zonally asymmetric rainfall change over tropical land. *Nat. Clim. Chang.* **8**, 434-440 (2018).

26. Richardson, T.B. et al. Carbon dioxide physiological forcing dominates projected eastern Amazonian drying. *Geophys. Res. Lett.* **45**, 2815-2825 (2018).
27. Zhou, S., Yu, B., Lintner, B., Findell, K.L., & Zhang, Y. Projected increase in global runoff dominated by land surface changes. *Nat. Clim. Chang.* **13**, 442-449 (2023).
28. Boysen, L.R. et al. Global climate response to idealized deforestation in CMIP6 models. *Biogeosciences* **17**, 5615-5638 (2020).
29. Luo, X. et al. The biophysical impacts of deforestation on precipitation: results from the CMIP6 model intercomparison. *J. Clim.* **35**, 3293-3311 (2022).
30. Lehner, F. et al. Partitioning climate projection uncertainty with multiple large ensembles and CMIP5/6. *Earth Syst. Dynam.* **11**, 491-508 (2020).
31. Nobre, C.A., Sampaio, G., Borma, L.S., Castilla-Rubio, J.C., Silva, J.S. and Cardoso, M. Land-use and climate change risks in the Amazon and the need of a novel sustainable development paradigm. *Proc. Natl. Acad. Sci. U.S.A.* **113**, 10759-10768 (2016).
32. Marengo, J.A. et al. Changes in climate and land use over the Amazon region: current and future variability and trends. *Front. Earth Sci.* **6**, 228 (2018).
33. Held, I.M. & Soden, B.J. Robust responses of the hydrological cycle to global warming. *J. Clim.* **19**, 5686-5699 (2006).
34. He, J. & Soden, B.J. A re-examination of the projected subtropical precipitation decline. *Nat. Clim. Chang.* **7**, 53-57 (2017).
35. Langenbrunner, B., Pritchard, M.S., Kooperman, G.J. & Randerson, J.T. Why does Amazon precipitation decrease when tropical forests respond to increasing CO2?. *Earth Future* **7**, 450-468 (2019).

36. Khanna, J., Medvigy, D., Fisch, G. & de Araujo Tiburtino Neves, T.T. Regional hydroclimatic variability due to contemporary deforestation in southern Amazonia and associated boundary layer characteristics. *J. Geophys. Res. Atmos.* **123**, 3993-4014 (2018).
37. Maeda, E.E., Abera, T.A., Siljander, M., Aragão, L.E., Moura, Y.M.D. & Heiskanen, J. Large-scale commodity agriculture exacerbates the climatic impacts of Amazonian deforestation. *Proc. Natl. Acad. Sci. U.S.A.* **118**, e2023787118 (2021).
38. Leite-Filho, A.T., Soares-Filho, B.S., Davis, J.L., Abrahão, G.M. & Börner, J. Deforestation reduces rainfall and agricultural revenues in the Brazilian Amazon. *Nat. Commun.* **12**, 1-7 (2021).
39. Spracklen, D.V. & Garcia-Carreras, L.J.G.R.L. The impact of Amazonian deforestation on Amazon basin rainfall. *Geophys. Res. Lett.* **42**, 9546-9552 (2015).
40. Sampaio, G. et al. CO_2 physiological effect can cause rainfall decrease as strong as large-scale deforestation in the Amazon. *Biogeosciences* **18**, 2511-2525 (2021).
41. Lawrence, D. & Vandecar, K. Effects of tropical deforestation on climate and agriculture. *Nat. Clim. Chang.* **5**, 27-36 (2015).
42. Jones, C.D. et al. C4MIP–The coupled climate–carbon cycle model intercomparison project: Experimental protocol for CMIP6. *Geosci. Model Dev.* **9**, 2853-2880 (2016).
43. Lawrence, D.M. et al. The Land Use Model Intercomparison Project (LUMIP) contribution to CMIP6: rationale and experimental design. *Geosci. Model Dev.* **9**, 2973-2998 (2016).

44. IPCC Summary for Policymakers. In: *Climate Change 2021: The Physical Science Basis. Contribution of Working Group I to the Sixth Assessment Report of the Intergovernmental Panel on Climate Change*. Cambridge Univ Press, Cambridge, United Kingdom and New York, NY, USA, 3-32 (2021).

45. Balch, J.K. et al. Warming weakens the night-time barrier to global fire. Nature 602, 442-448 (2022).

46. Jain, P., Castellanos-Acuna, D., Coogan, S.C.P., Abatzoglou, J.T., & Flannigan, M.D. Observed increases in extreme fire weather driven by atmospheric humidity and temperature. *Nat. Clim. Chang.* **12**, 63-70 (2022).

47. Cheng, L. et al. Past and future ocean warming. *Nat. Rev. Earth Environ.* **3**, 776-794 (2022).

48. Stickler, C.M. et al. The potential ecological costs and cobenefits of REDD: a critical review and case study from the Amazon region. *Glob. Change Biol.* **15**, 2803-2824 (2009).

49. Zemp, D.C. et al. Self-amplified Amazon forest loss due to vegetation-atmosphere feedbacks. *Nat. Commun.* **8**, 1-10 (2017).

50. Norby, R.J. et al. Model–data synthesis for the next generation of forest free-air CO_2 enrichment (FACE) experiments. *New Phytol.* **209**, 17-28 (2016).

51. Medlyn, B.E. et al. Stomatal conductance of forest species after long-term exposure to elevated CO2 concentration: a synthesis. *New Phytol.* 149, 247-264 (2008).

52. Baker, J.C.A. & Spracklen, D.V. Divergent representation of precipitation recycling in the Amazon and the Congo in CMIP6 models. *Geophys. Res. Lett.* E2021GL095136 (2022).

53. Wills, R.C.J., Dong, Y., Proistosecu, C., Armour, K.C., Battisti D.S. Systematic climate model biases in the large-scale patterns of recent sea-surface temperature and sea-level pressure change. *Geophys. Res. Lett.* **49**, e2022GL100011 (2022).

54. Barichivich, J. et al. Recent intensification of Amazon flooding extremes driven by strengthened Walker circulation. *Sci. Adv.* **4**, eaat8785 (2018).

55. Weijer, W., Cheng, W., Garuba, O.A., Hu, A., Nadiga, B.T. CMIP6 models predict significant 21st century decline of the Atlantic Meridional Overturning Circulation. *Geophys. Res. Lett.* **47**, e2019GL086075 (2020).

56. Ciemer, C., Winkelmann, R., Kurths, J., & Boers, N. Impact of an AMOC weakening on the stability of the southern Amazon rainforest. *Eur. Phys. J. Spec. Top.* **230**, 3065-3073 (2021).

57. Cai, X. et al. Improving representation of deforestation effects on evapotranspiration in the E3SM land model. *J. Adv. Model. Earth Syst.* **11**, 2412-2427 (2019).

58. Chen, L. & Dirmeyer, P.A. Reconciling the disagreement between observed and simulated temperature responses to deforestation. *Nat. Commun.* **11**, 1-10 (2020).

59. Windisch, M.G., Davin, E.L. & Seneviratne, S.I. Prioritizing forestation based on biogeochemical and local biogeophysical impacts. *Nat. Clim. Chang.* **11**, 867-871 (2021).

60. Bright, R.M., Davin, E., O'Halloran, T., Pongratz, J., Zhao, K. & Cescatti, A. Local temperature response to land cover and management change driven by non-radiative processes. *Nat. Clim. Chang.* **7**, 296-302 (2017).

61. Duveiller, G., Hooker, J. & Cescatti, A. The mark of vegetation change on Earth's surface energy balance. *Nat. Commun.* **9**, 1-12 (2018).

62. Gillet, N.P. et al. The Detection and Attribution Model Intercomparison Project (DAMIP v1.0) contribution to CMIP6. *Geosci. Model Dev.* **9**, 3685–3697 (2016).

Cited in methods:

63. Schulzweida, U. Climate data operators (CDO) user guide (Version 1.9.8). https://doi.org/10.5281/zenodo.3539275 (2019).

64. Wu, T. et al. The Beijing Climate Center climate system model (BCC-CSM): the main progress from CMIP5 to CMIP6. *Geosci. Model Dev.* **12**, 1573–1600 (2019).

65. Swart, N. C. et al. The Canadian Earth System Model version 5 (CanESM5. 0.3). *Geosci. Model Dev.* **12**, 4823–4873 (2019).

66. Danabasoglu, G. et al. The Community Earth System Model version 2 (CESM2). *J. Adv. Model Earth Syst.* **12**, e2019MS001916 (2020).

67. Séférian, R. et al. Evaluation of CNRM Earth System Model, CNRM-ESM2-1: role of earth system processes in present-day and future climate. *J. Adv. Model Earth Syst.* **11**, 4182–4227 (2019).

68. Boucher, O. et al. Presentation and evaluation of the IPSL-CM6A-LR climate model. *J. Adv. Model Earth Syst.* **12**, 1–52 (2020).

69. Kelley, M. et al. GISS-E2. 1: configurations and climatology. *J. Adv. Model Earth Syst.* **12**, e2019MS002025 (2020).

70. Sellar, A. A. et al. Implementation of UK Earth system models for CMIP6. *J. Adv. Model Earth Syst.* **12**, e2019MS001946 (2020).

71. Mauritsen, T. et al. Developments in the MPI-M Earth System Model version 1.2 (MPI-ESM1. 2) and its response to increasing CO_2. *J. Adv. Model Earth Syst.* **11**, 998–1038 (2019).

72. Hurtt, G.C. et al. Harmonization of global land use change and management for the period 850–2100 (LUH2) for CMIP6. *Geosci. Model Dev.* **13**, 5425-5464 (2020).